Electrochemistry
The Electrochemical Society of Japan
Received: August 26, 2022
Accepted: October 18, 2022
Published online: October 21, 2022
Issued: November 17, 2022
https://doi.org/10.5796/electrochemistry.22-00099
https://doi.org/10.50892/data.electrochemistry.21365886
Article
Electrochemistry, **90(11)**, 117004 (2022)

Anion-dominated Redox Reaction of a SAM of an Alkylthiolated Viologen Bearing a Covalently-attached Intramolecular Sulfonate Group on a Gold Electrode

Masaki TOYOHARA[a] and **Takamasa SAGARA**[b,*,§]

[a] *Department of Advanced Technology and Science for Sustainable Development, Graduate School of Engineering, Nagasaki University, 1-14 Bunkyo, Nagasaki 852-8521, Japan*
[b] *Division of Chemistry and Materials Sciences, Graduate School of Engineering, Nagasaki University, 1-14 Bunkyo, Nagasaki 852-8521, Japan*

* *Corresponding author: sagara@nagasaki-u.ac.jp*

ABSTRACT

The redox processes of the self-assembled monolayers (SAMs) of alkylthiolated viologens on Au electrodes are largely determined by oxidation-state-dependent binding of electrolyte anions to the viologen moiety in an aqueous solution. In this paper, we give an answer to a question: what if the SAM-forming molecule has a covalently-attached intermolecular anionic site? We used the results of the voltammetric measurements for a SAM of a viologen with a covalently-attached sulfonate group, 1-(10-mercaptodecyl)-1′-(3-sulfonatopropyl)-4,4′-bipyridinium bromide (HS-C10-V-C3-SO_3^- bromide salt), and examined the effect of intramolecular ion binding on the redox behavior. We found the coexistence of two distinct types of redox couples: one with a viologen moiety, which binds always to the sulfonate group, and the other with a moiety, which catches and releases an electrolyte anion from the solution upon redox. We deciphered rather complicated behavior and discussed the implications.

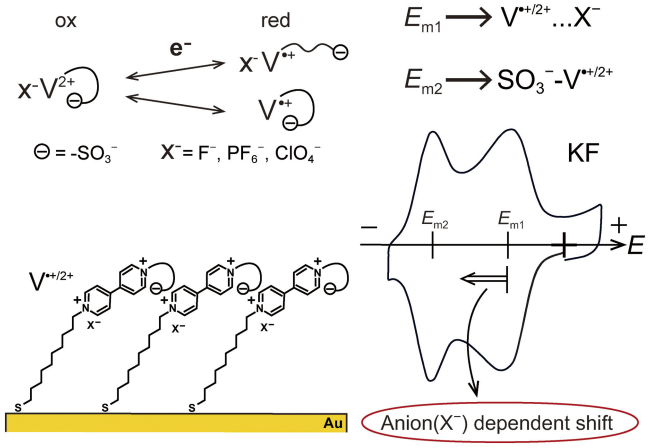

Keywords : Alkylthiolated Viologen Monolayer, Anion Effect, Electrostatic Binding, Ion-pair Formation

1. Introduction

The redox reactions of electro-active organic monolayers confined on electrode surfaces are often affected by the properties and concentration of counter ions in the electrolyte solution. When a self-assembled monolayer (SAM) on an electrode surface has a cationic redox active site such as the oxidized form of a ferrocenyl group (Fc), the binding of anions coming from the electrolyte solution phase to the cationic site largely determines the redox behavior.[1–9] When the cationic redox active site is a viologen moiety, the anion binding occurs to both oxidized and reduced forms and affects the redox behavior significantly.[10–19] For the Fc group at the alkyl terminal position[1–9] or viologen moiety at the midway of the alkyl chain,[10–19] their formal potentials of the one-electron redox process ($E^{o\prime}$) shift to negative to a greater extent when a more strongly bound anion participates. In an ideal condition, $E^{o\prime}$ shifts to negative by ca. 59 mV per one decade increase of the anion concentration at room temperature.[1,11,20] The strength of the anion binding and therefore the binding equilibrium is determined by the hydration number or the softness of the anion; the more strongly bound anion has a smaller hydration number or a larger softness. The potential shift applies to the anion sensing. For the fabrication of such a sensor, we must prepare a well-ordered SAM structure with a unique ion-binding site and a suitable micro-environment. The designs of the SAM-forming molecules and the SAM structure should be optimized. Especially, the settings of alkyl chain lengths,[7,8,11–16] the orientation of the redox moiety,[12,13] the superficial density of the SAM forming molecules on the electrode surface,[9] and the properties of the electrode surface[17] are of profound importance.

Many studies have focused on the cases where all the bound anions come from the bulk of electrolyte solution. Then, what if an anionic site is covalently-attached intramolecularly to the SAM-forming molecule? We assume the SAM-forming molecule has one viologen site that is accompanied by a covalently-attached anion site. Recall that the oxidized form of viologen is dication (V^{2+}) and the one-electron reduced form is monocation monoradical ($V^{\bullet+}$). When all the viologens in the SAM are one-electron reduced, half the total number of counter anions at most are of covalently-attached ones, while the rest of them come from the solution phase (Fig. 1). If the intramolecular anion site is capable of strong binding to a viologen moiety, the viologen-anion ion-pairs have various combinations of bound anions. The situation may be complicated, but it provides us additionally with rich control factors of the redox behavior of the SAMs.

We aim to unveil the binding behavior of the covalently-attached intramolecular anion site in the SAM to the viologen therein at a Au electrode in aqueous electrolyte solutions. To the best of our

§ECSJ Active Member
M. Toyohara orcid.org/0000-0001-7971-6252
T. Sagara orcid.org/0000-0002-7975-394X

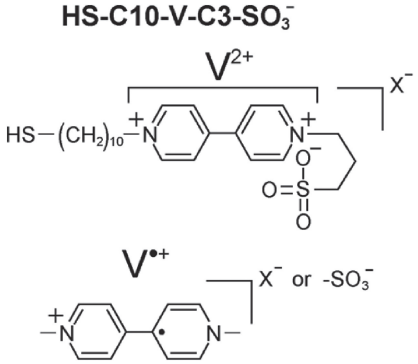

Figure 1. Molecular structure and redox states of 1-(10-mercaptodecyl)-1′-(3-sulfonatopropyl)-4,4′-bipyridinium (HS-C10-V-C3-SO_3^-) bromide.

knowledge, the ion binding between a cationic redox center and a covalently-attached intramolecular anion site has never been studied in any redox-active SAM. In this work, we use an alkylthiolated viologen with a 3-sulfonatopropyl group as a side substituent, 1-(10-mercaptodecyl)-1′-(3-sulfonatopropyl)-4,4′-bipyridinium (HS-C10-V-C3-SO_3^-) bromide, shown in Fig. 1, as the SAM-forming molecule. Its SAM has ω-sulfonate sites. In Fig. 1, we assume that the bending of the intervening propyl chain makes it possible for the sulfonate group to come in proximity to the pyridinium cationic nitrogen site, resulting in the formation of an ion-pair. Li and coworkers obtained a ^{1}H NMR NOESY spectrum, in which the nuclear Overhauser effect demonstrated the above-mentioned type of ion-pair formation in 1,1′-bis(3-sulfonatopropyl)-4,4′-bipyridinium dibromide in the aqueous solution phase.[21] Their DFT calculation also supported this conformation.

2. Experimental

2.1 Materials

A poly-crystalline Au disk electrode with a geometrical area of $A = 0.0201\ \mathrm{cm}^2$ with a PEEK resin sheath was purchased from BAS Co. It was polished with a 0.3 µm and then a 0.05 µm alumina slurry to a mirror finish, sonicated for 1 min each in acetone and water, and then rinsed. Its oxidation-reduction cycle (ORC) pretreatment in 0.1 M $HClO_4$ was followed by the SAM formation procedure. HS-C10-V-C3-SO_3^- bromide salt was home-synthesized as shown in Scheme S1. Water was purified through a Milli-Q integral (Millipore) to a resistivity >18 MΩ cm. All the salts were of commercially available reagent grade and used without further purification.

2.2 SAM formation procedure

HS-C10-V-C3-SO_3^- bromide salt was dissolved in methanol to prepare its 13.3 mM solution (M ≡ mol dm^{-3}). The ORC-treated Au electrode was immersed in the solution for 24 h at room temperature in the dark. It was rinsed with methanol, water, and the electrolyte solution to be used first, and set in the electrochemical cell filled with the deaerated electrolyte solution.

2.3 Voltammetric measurements

Cyclic voltammograms (CVs) were measured in a three-electrode configuration. A Ag|AgCl electrode in saturated KCl solution was used as the reference electrode. A coiled Au wire served as the counter electrode. All the measurements were conducted in an argon gas atmosphere at 23 ± 2 °C using a potentiostat (Huso, HECS 315B). When replacing one electrolyte salt solution with another, the cell was rinsed well with water and then by the next solution before pouring it.

3. Results and Discussion

3.1 Model of possible redox processes

Both electrolyte anion and covalently-attached anion site to the SAM-forming viologen molecule may participate in multiple elementary redox processes. The possible redox processes are modeled in Fig. 2.

Recall that the $E^{o\prime}$ of the redox reaction of viologen in the SAM in the presence of electrolyte anion, X^-, which can bind to the viologen site, is described[11,17–19] as

$$E^{o\prime} = E_1 + \frac{RT}{n_a F}\ln\frac{K_{\mathrm{Red}}}{K_{\mathrm{Ox}}} - \frac{RT}{n_a F}\ln[\mathrm{X}^-] \qquad (1)$$

where E_1 is the standard redox potential of $V^{\bullet+}/V^{2+}$ couple, n_a is the apparent number of electrons involved in the redox equilibrium, R is the gas constant, F is the Faraday constant, T is the temperature, and K_{Ox} and K_{Red} are the equilibrium constants describing the anion binding processes:

$$V^{2+} + 2X^- = V^{2+}\ldots 2X^- \quad K_{\mathrm{Ox}}$$
$$V^{\bullet+} + X^- = V^{\bullet+}\ldots X^- \quad K_{\mathrm{Red}}$$

Processes 1 and 3 in Fig. 2 involve the binding of electrolyte anion X^- to the viologen site and its liberation. These processes depend on the nature and concentration of X^- as represented by Eq. 1. Meanwhile, Processes 2, 4, and 5 in Fig. 2 involve the binding of the covalently-attached sulfonate ion site and its liberation, regardless of whether the ion site is of the identical SAM-forming molecule or its neighbor. The close proximity of sulfonate group to the quaternary nitrogen of viologen in the same molecule (Fig. 1) was confirmed in D_2O solution by our own measurements of NOESY for HS-C10-V-C3-SO_3^- bromide (Fig. S1).

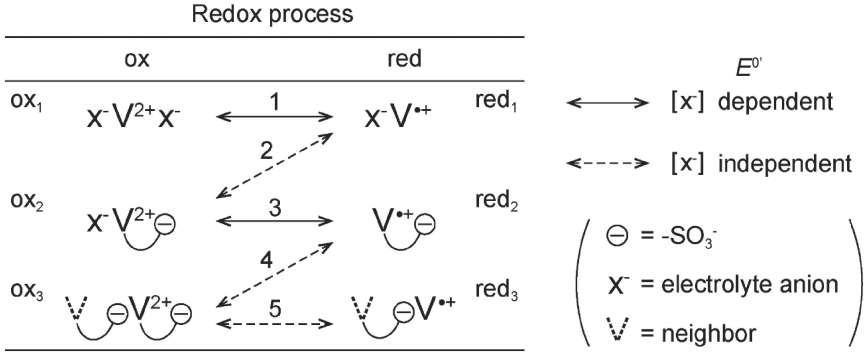

Figure 2. Possible redox processes of HS-C10-V-C3-SO_3^--SAM in electrolyte solution containing an anion X^-, which has binding activity to both V^{2+} and $V^{\bullet+}$.

Taken together, we can predict the following features of the voltammetric behavior:

- Processes 4 and 5 are indistinguishable in CV when the binding strength to a viologen moiety is the same for the sulfonate attached to the identical SAM-forming molecule and the sulfonate attached to the neighbor.
- Unless the electrolyte anion X^- affects the binding properties of the covalently-attached sulfonates, Processes 2, 4, and 5 are independent of the solution concentration of X^-. Therefore, they give constant, X^--independent redox potentials in CV, even if peak current were to change.

3.2 Voltammograms in KF solution

For a freshly prepared HS-C10-V-C3-SO_3^--SAM on an Au electrode, CV measurements were made in 50 mM KF solutions. F^- binds most weakly to viologen in the SAM in an aqueous solution among ever-tested inorganic anions.[12,18,19] The initial scan CV (curve a in Fig. 3) changed to a steady state CV (curve b) after continuous potential scanning for over 15 min. The peak currents of all four peaks of the curve b were proportional to the scan rate (v) in the range of 25 to 200 mV s^{-1}, indicative of the occurrence of a surface-confined redox processes of the $V^{\bullet+}/V^{2+}$ couples. Two peak pairs are evident: Peak pair-I at the less-negative midpoint potential of $E_{m1} = -217$ mV and Peak pair-II at the more negative midpoint potential of $E_{m2} = -531$ mV with narrower peak width than the former. The peak separations between anodic and cathodic peaks, ΔE_p, of both pairs were 5 mV at $v = 50$ mV s^{-1}, indicating high reversibility of the redox reaction and rigid SAM structure against the potential change. We used the shadowed areas of the cathodic and anodic peaks in Fig. 3, Q, to calculate the amount of immobilized viologen as being $\Gamma = 3.5 \pm 0.15 \times 10^{-10}$ mol cm^{-2} as the average and deviation of three runs.

The value of E_{m1} is less-negative as the redox potential of a $V^{\bullet+}/V^{2+}$ couple than that of 1′-bis(3-sulfonatopropyl)-4,4′-bipyridinium dibromide in aqueous solution reported as being −597 mV vs. Ag|AgCl-sat KCl.[21,22] However, the SAM of a typical alkylthiolated viologen, 1-pentyl-1′-(11-mercapto)undecyl-4,4′-bipyridinium, on a Au electrode showed $E_m = -192$ mV in 0.1 M KF solution.[18]

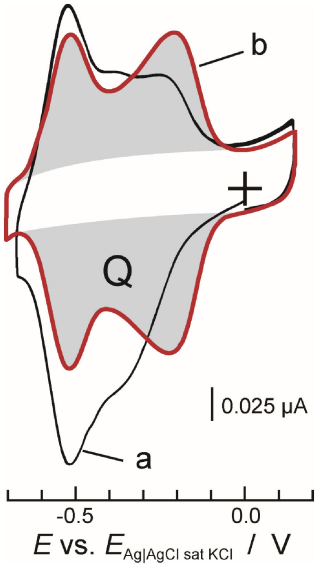

Figure 3. CVs for a HS-C10-V-C3-SO_3^--covered Au electrode in 50 mM KF aqueous solution at $v = 50$ mV s^{-1}. Curve a (black line) represents the initial scan after dipping the electrode in the electrolyte solution and curve b (red line) does the CV after potential sweeping for over 15 min until steady-state was reached. The amount of electronic charge corresponding to the cathodic gray-shadowed area was labelled as "Q".

Therefore, to the redox potential of a viologen with no interaction with sulfonate, E_{m1} is assigned. The above-mentioned value of Γ corresponds to the average distance between the immobilized molecules of 0.52 nm, assuming the two-dimensional closest packing. Because the molecules are most likely tilted from the surface normal,[17,19] this distance indicates that the ion-pair formation of a viologen unit with a sulfonate group of a neighbor molecule, namely the existence of ox3 and red3 in Fig. 2, is permittable. In the process of the SAM formation, the covalently-attached sulfonate groups may have acted as counter anions through electrostatic interaction with viologen sites to reduce electrostatic repulsion between neighboring viologens, resulting in the above-mentioned value of Γ, which is greater than that of the SAM of 1-(10-mercaptodecyl)-1′-methyl-4,4′-bipyridinium.[17]

Our interpretation of the CV in Fig. 3 in light of Fig. 2 is as follows. Peak pair-I originates from Processes 1 and 3 in Fig. 2 where X^- is F^-, because it has less-negative $E^{o\prime}$ than that of propyl-sulfonate-substituted viologen[21,22] in the solution phase. Although the binding of F^- to the viologen moiety is weak, its binding equilibrium in the present SAM gives $K_{red}[F^-]$ or $K_{ox}[F^-]$ values much higher than unity, resulting in the apparent contribution of the third term of the r.h.s. of Eq. 1.[17,19] Peak pair-II originates from Processes 4 and 5, because the E_{m2} value was independent of time, its peak current, and the change of the peak potentials and currents of Peak pair-I. Because of the weakness of the binding of F^- from the electrolyte solution compared to the binding of in-SAM sulfonate, we exclude Process 2. To confirm these interpretations, we show the results of examinations of the addition of various anions and the concentration dependence in sections 3.3–3.6.

In the period of 15 min until the CV reached a steady state, the change of the curve shape from curve a to b was monotonic. One counter anion when the SAM was formed is bromide. The need for such a long time indicates that it is a sluggish process to liberate the bromide ion to the bulk of the solution and to reach the steady anion-distribution state and corresponding SAM structure.

3.3 KF concentration dependence

CVs at various concentrations of KF were recorded, and the steady-state CVs at three typical concentrations are shown in Fig. 4. In 5 mM and 500 mM solutions, the peak currents were proportional to v for all peaks as with the data in 50 mM KF (Fig. 3). The concentration dependence data revealed that E_{m1} obviously shifts

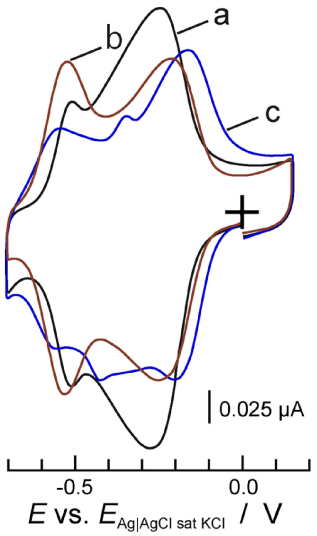

Figure 4. CVs for a HS-C10-V-C3-SO_3^--covered Au electrode at $v = 50$ mV s^{-1} in KF solutions of three concentrations: 500 mM (curve a, black line), 50 mM (curve b, red line), and 5 mM (curve c, blue line).

to more negative with increasing KF concentration, whereas E_{m2} slightly shifts to positive. With increasing KF concentration, the transferal of peak charge from Peak pair-II to Peak pair-I became greater while keeping the total charge almost constant, and therefore the peak current ratio in Fig. 4 has changed. Higher concentrations of KF enhance the electrostatic shielding. In particular, the electrostatic ion-pair, $V^{2+}\ldots SO_3^-$, where the sulfonate is of covalently-attached one to the SAM, suffers by weakening the interaction. It turns out that, at the high KF concentration, the percentage of the presence of states ox2, ox3, red2, red3 (Fig. 2) may decrease. Some fractions of sulfonate are liberated from viologen site and mobile in the solution phase while attached to viologen through motile propyl chain. This may decrease the occurrence of redox processes that accompanies sulfonate ion binding, resulting in the decrease of peak current of Peak pair-II.

In Fig. 4, E_{m1} shifted to more negative with increasing KF concentration, and the shift has roughly a slope of −40 mV/decade. Although the binding of F^- to viologen in the SAM is weak, the binding affected the voltammetric response as noted in the previous section.

These results made it clear that Peak pair-II is ascribed to the Processes 4 or 5, while Peak I is presumably due to Processes 1 or 3 (Fig. 2). At 500 mM, Peak pair-I gave greater peak currents than Peak pair-II. The smaller Peak pair-II may originate from the fact that the binding between viologen and sulfonate group is shielded by the high salt concentration of KF. At 5 mM, new peaks were observed in between Peak pairs-I and -II. Presumably, under very low ionic strength, the binding pattern of sulfonate to viologen moiety has diversified. Because of this new complexity, we will not discuss the situation of such a low salt concentration any more in the present paper.

3.4 Tetramethylammonium fluoride concentration dependence

Further examination of voltammetric behavior was made by adding tetramethylammonium fluoride, $Me_4N^+F^-$, to the electrolyte solution. We expected that Me_4N^+ competes against the viologen site for binding with the sulfonate site in the SAM. Because Me_4N^+ is an organic cation with minimal alkyls, its interaction with the sulfonate site is predominately electrostatic. The results of the measurements with various concentrations of $Me_4N^+F^-$ are shown in Fig. 5. In these measurements, the ionic strength of the electrolyte solution and F^- concentration were kept constant by adding KF to avoid the complexity discussed in section 3.3.

The three CVs in Fig. 5 showed E_{m1} at −315 ± 25 mV and a shoulder at −465 ± 5 mV. In all the CVs, the peak currents were proportional to v in the range of 25 to 200 mV s^{-1}. Comparison of these CVs with the CV in 500 mM KF (Fig. 4) shows that the presence of only 5 mM $Me_4N^+F^-$ changed Peak pair-II to be a shoulder, indicative of the decrease in the number of sulfonate group that binds to viologen because of the effect of Me_4N^+ predicted above. However, the effect leveled off; the CV shape shows no further change along with the increase of $Me_4N^+F^-$ concentration up to 500 mM.

3.5 Effects of the addition of alkyl sulfates

Alkyl sulfate surfactants bind to alkylthiolated viologen SAM strongly as demonstrated in our previous publication; the alkyl chain-chain interaction between the surfactant and the SAM-forming molecule enhances the interaction effectively in addition to the electrostatic binding between viologen and sulfate head group in a low electric permittivity environment of the alkyl phase in the SAM.[19] The intent of adding alkyl sulfates in the present system as X^- (Fig. 2) is to see their enhanced binding to the viologen moiety in the SAM.

As shown in Fig. 6, all three alkyl sulfates gave Peak pair-II dominantly, in sharp contrast to F^- rich media (Figs. 3 and 4), with a midpoint potential around −0.50 V. At the less-negative side to the Peak pair-II, methyl sulfate gave a shoulder around −0.27 V instead of Peak pair-I, and so did octyl sulfate a smaller shoulder. In dodecyl sulfate solution, regardless of whether the paired anion is the covalently-attached sulfonate or dodecyl sulfate from the solution phase, almost all V^{2+} has two strongly bound anions and all $V^{\bullet+}$ have one strongly bound anion, resulting in solely the peak at −0.50 V without a shoulder. For all three alkyl sulfates, the peak waveform was symmetrical with respect to both potential axis and peak potential, and peak currents were proportional to v. The waveform was sharper as the length of the alkyl chain increases. The time course change such as observed in Fig. 3 was not seen. The amounts of redox-active viologen for curves b and c is ca. 15 % less than the amount for curve a, which was measured at the beginning among the three curves in Fig. 6. It is likely that, upon the binding of the long-chain surfactants, some viologen moieties were buried deep in the thus-formed thick alkyl region. This may inhibit water and anion permeation. The appearance of such mechanism must be confirmed in the future. These results indicate that the binding between alkyl sulfate and viologen is strong and stable. The binding

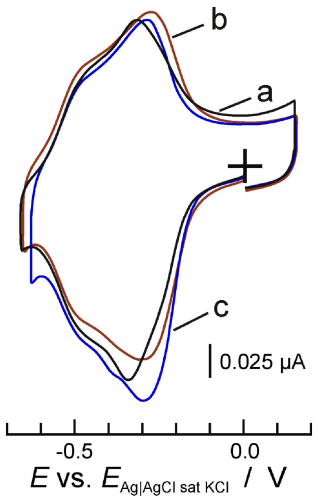

Figure 5. CVs for a HS-C10-V-C3-SO_3^--covered Au electrode at v = 50 mV s^{-1} in ($Me_4N^+F^-$ + KF) mixed aqueous solutions: 5 mM $Me_4N^+F^-$ and 495 mM KF (curve a, black line), 50 mM $Me_4N^+F^-$ and 450 mM KF (curve b, red line), and 500 mM $Me_4N^+F^-$ (curve c, blue line).

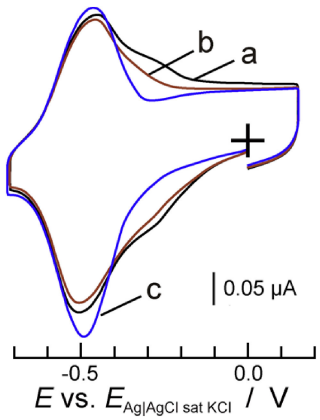

Figure 6. CVs for a HS-C10-V-C3-SO_3^--covered Au electrode at v = 50 mV s^{-1} in (50 mM alkyl sulfate sodium salt + 50 mM KF) mixed aqueous solutions. The alkyl sulfates used are $CH_3OSO_3^-Na^+$ (curve a, black line), $CH_3(CH_2)_7OSO_3^-Na^+$ (curve b, red line), and $CH_3(CH_2)_{11}OSO_3^-Na^+$ (curve c, blue line).

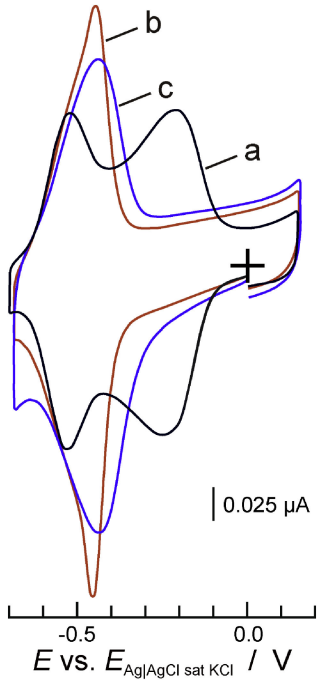

Figure 7. CVs for a HS-C10-V-C3-SO_3^--covered Au electrode at $v = 50\,\mathrm{mV\,s^{-1}}$ in 50 mM KF (curve a, black line), 50 mM KPF_6 (curve b, red line), and 50 mM $KClO_4$ (curve c, blue line).

of F^- present in the solution was suppressed by methyl and octyl sulfates and completely excluded by dodecyl sulfate while all X^- in Fig. 2 is the alkyl sulfate.

3.6 Effects of the addition of hydrophobic inorganic anions

In Fig. 7, the CVs in electrolyte salt solutions of the anions with high softness were compared with the CV in a KF solution. In the three electrolyte solutions, all the peak currents were proportional to v in the range of 25 to 200 $\mathrm{mV\,s^{-1}}$, indicative of the occurrence of surface-confined redox processes of the $V^{\bullet+}/V^{2+}$ couples. Only one pair of sharp peaks was observed in each of $KClO_4$ and KPF_6 solutions of 50 mM concentration. Peak pair-I shifted to negative and merged with Peak pair-II. The midpoint potential of the merged peak in $KClO_4$ solution was at −440 mV and that in KPF_6 solution was at −455 mV. These values are slightly more positive than E_{m2} in 50 mM KF solution. These results represent that binding of external anions to viologen is dependent on the hydration number or softness also in this SAM. Most likely, Processes 1, 2, and 3 (Fig. 2) take place with ClO_4^- and PF_6^- as X^-, and these processes have redox potentials slightly more positive than that for Process 5. The symmetry of the peaks is very high. ΔE_p was smaller than 12 mV in the presence of $KClO_4$ and KPF_6, whereas it was over 100 mV for previously reported alkylthiolated viologen SAMs with a viologen moiety positioned in the middle of the alkyl chain.[11,18] Presumably, the presence of in-SAM sulfonates suppress the conformational change of the SAM upon redox reaction. As we reported previously, the binding of highly hydrophobic PF_6^- to the viologen site in the SAM produced very sharp peaks.[11,18] The sharpness was observed for curve b in Fig. 7, even though the peak is the superposition of Peak pairs I and II. This may be due to the predominant occurrence of Process 2 in Fig. 2 with $X^- = PF_6^-$ at the observed peak.

3.7 Significance of the presence of covalently-attached sulfonate in the SAM

We found that the redox behavior of the SAM of alkylthiolated viologen bearing a covalently-attached sulfonate group in the SAM differs from the previously reported SAMs without any attached anion site. The highlighted difference is that the former showed multiple anion binding processes, not only the softness-dependent binding of anions from the electrolyte solution phase but also binding processes involving the covalently-attached anion. These processes were reflected in the redox behavior as observed as voltammetric responses. The viologen moieties in the SAM showed highly reversible redox reactions even under intensive binding interaction with the covalently-attached anion sites. This may originate from the rigidity of the SAM structure against potential changes. In the solution where only KF was dissolved, two pairs of redox peaks were observed (Figs. 3 and 4). One was assigned to the redox with weak binding of F^- to viologen and other was that with strong binding of the covalently-attached sulfonate to viologen. For the latter, high concentrations KF give rise to shielding of the electrostatic interaction and weaken the binding (Fig. 4). In cationic tetramethylammonium fluoride solutions, the interaction of ammonium in solution with the covalently-attached sulfonate is in competition with the interaction of viologen with covalently-attached sulfonate, although the effect is limited (Fig. 5). In the presence of both alkyl sulfate and F^- in the solution phase, the binding F^- with viologen was annihilated, and the extent was severer with the sulfate ion with longer alkyl chain (Fig. 6). In the solution of inorganic potassium salts with highly hydrophobic anions such as $KClO_4$ and KPF_6, ClO_4^- and PF_6^- interact closely to viologen sites, although the binding of covalently-attached sulfonate with viologen remains (Fig. 7). To sum up, all the observed behavior is governed by the binding strength balance and competition between X^- and covalently-attached sulfonate to the viologen moiety (Fig. 2).

4. Conclusions

The redox behavior of viologen with a covalently-attached sulfonate group in the SAM showed electrolyte anion-dependent anion binding features as shown in Fig. 2. Irrespective of the properties of the electrolyte anion, redox process of viologen associated with the binding to the sulfonate was observed in any case. Long-chain alkyl sulfates bind strongly even to the viologen moiety bearing covalently-attached sulfonate group. The electrostatic interaction between the viologen and covalently-attached sulfonate in the SAM is strong, though it is balanced by the electrostatic shielding in high ionic strength conditions and the presence of highly hydrophobic anions. This study has uncovered an important factor, the incorporation of covalently-attached anions in the SAM. It determines the electrolyte anion binding processes and thus the redox behavior of the redox-active SAMs. It emerges as a new strategy for the development of the functions of SAMs on electrode surfaces, provided that future studies clarify the ion-pair conformation at a molecular level in the SAMs.

Acknowledgments

We thank financial supports by the Grant-in-Aid of Scientific Research on Innovative Area “Molecular Engine” (JP21H00407) to TS from MEXT of Japan.

CRediT Authorship Contribution Statement

Masaki Toyohara: Conceptualization (Equal), Data curation (Lead), Formal analysis (Lead), Investigation (Lead), Methodology (Lead), Visualization (Lead), Writing – original draft (Lead), Writing – review & editing (Equal)

Takamasa Sagara: Conceptualization (Equal), Funding acquisition (Lead), Project administration (Lead), Supervision (Lead), Writing – review & editing (Equal)

Data Availability Statement

The data that support the findings of this study are openly available under the terms

Conflict of Interest

The authors declare that they have no known competing financial interests or personal relationships that could have appeared to influence the work reported in this paper.

Funding

Ministry of Education, Culture, Sports, Science and Technology (MEXT) of Japan: the Grant-in-Aid of Scientific Research on Innovative Area "Molecular Engine": JP21H00407

References

D1. M. Toyohara and T. Sagara, *J-STAGE Data*, https://doi.org/10.50892/data.electrochemistry.21365886, (2022).
1. K. Uosaki, Y. Sato, and H. Kita, *Langmuir*, **7**, 1510 (1991).
2. T. Kondo, M. Okamura, and K. Uosaki, *J. Organomet. Chem.*, **637–639**, 841 (2001).
3. G. Valincius, G. Niaura, B. Kazakevičienė, Z. Talaikytė, M. Kažemėkaitė, E. Butkus, and V. Razumas, *Langmuir*, **20**, 6631 (2004).
4. A. V. Rudnev, U. Zhumaev, T. Utsunomiya, C. Fan, Y. Yokota, K.-I. Fukui, and T. Wandlowski, *Electrochim. Acta*, **107**, 33 (2013).
5. R. A. Wong, Y. Yokota, M. Wakisaka, J. Inukai, and Y. Kim, *Nat. Commun.*, **11**, 4194 (2020).
6. T. J. Duffin, N. Nerngchamnong, D. Thompson, and C. A. Nijhuis, *Electrochim. Acta*, **311**, 92 (2019).
7. A. S. Viana, A. H. Jones, L. M. Abrantes, and M. Kalaji, *J. Electroanal. Chem.*, **500**, 290 (2001).
8. N. Nerngchamnong, D. Thompson, L. Cao, L. Yuan, L. Jiang, M. Roemer, and C. A. Nijhuis, *J. Phys. Chem. C*, **119**, 21978 (2015).
9. L. Y. S. Lee, T. C. Sutherland, S. Rucareanu, and R. B. Lennox, *Langmuir*, **22**, 4438 (2006).
10. H. C. De Long and D. A. Buttry, *Langmuir*, **6**, 1319 (1990).
11. T. Sagara, H. Maeda, Y. Yuan, and N. Nakashima, *Langmuir*, **15**, 3823 (1999).
12. S. L. Hiley and D. A. Buttry, *Colloids Surf., A*, **84**, 129 (1994).
13. X. Tang, T. W. Schneider, J. W. Walker, and D. A. Buttry, *Langmuir*, **12**, 5921 (1996).
14. H. C. De Long and D. A. Buttry, *Langmuir*, **8**, 2491 (1992).
15. J. Yan, J. Li, W. Chen, and S. Dong, *J. Chem. Soc., Faraday Trans.*, **92**, 1001 (1996).
16. B.-Y. Wen, J.-S. Lin, Y.-J. Zhang, P. M. Radjenovic, X.-G. Zhang, Z.-Q. Tian, and J.-F. Li, *J. Am. Chem. Soc.*, **142**, 11698 (2020).
17. T. Sagara and M. Toyohara, *J. Electroanal. Chem.*, **919**, 116514 (2022).
18. T. Sagara, H. Tsuruta, and N. Nakashima, *J. Electroanal. Chem.*, **500**, 255 (2001).
19. T. Sagara, Y. Hagi, and M. Toyohara, *Langmuir*, **38**, 979 (2022).
20. A. J. Bard and L. R. Faulkner, *Electrochemical Methods: Fundamentals and Applications* (2nd ed.), John Wiley & Sons, Inc., New York (2001).
21. H. Li, H. Fan, B. Hu, L. Hu, G. Chang, and J. Song, *Angew. Chem., Int. Ed.*, **60**, 26971 (2021).
22. A. Badalyan, Z.-Y. Yang, B. Hu, J. Luo, M. Hu, T. L. Liu, and L. C. Seefeldt, *Biochemistry*, **58**, 4590 (2019).